

# Raman Measurements of the Stabilization Process of a Lifted Flame Tuned by Acoustic Excitation

Yei-Chin Chao<sup>1</sup>, Chih-Yung Wu<sup>1</sup>, Tony Yuan<sup>1</sup>, and Tsarng-Sheng Cheng<sup>2</sup>

<sup>1</sup>Institute of Aeronautics and Astronautics,  
National Cheng Kung University,  
Tainan 701, TAIWAN, ROC

<sup>2</sup>Department of Mechanical Engineering,  
Chung-Hua University,  
Hsin-Chu 300, TAIWAN, ROC

## Introduction

For several decades, the stabilization mechanism of lifted jet diffusion flames has attracted intensive research attentions [1]. The stabilization of a lifted flame illustrates most of the important features of flame-flow interactions and flame stability characteristics. It is generally accepted [2] that except for a small distance next to the flame base, upstream of the lifted flame is cold flow and is dominated by the near-field large-scale coherent structures of the jet flow. Usually the lifted flame remains lifted until the exit velocity is reduced to a value well below its original liftoff velocity. This is the hysteresis phenomenon. The importance of large scale structures on the dynamic behavior of flame stability were carefully investigated [3, 4, 5, 6] and Chao and Jeng [7] also showed the feasibility of using external acoustic excitation to control the hysteresis phenomenon. As discussed above [7, 2], lifted flames properly tuned by external acoustic excitation will exhibit periodic oscillation at the flame base, with the flame base moving downstream and propagating upstream in an oscillatory cycle. Therefore, this acoustically tuned liftoff flame is ideal for the detailed measurements of the scalar quantities using the line Raman spectroscopy technique, which is usually single shot with low repetition, to delineate the stabilization process and to verify the various theories and findings concerning the stabilization mechanism. This motivates the current study.

## Experimental Setup

The experimental setup, the Raman system, and the measurement locations for the line Raman segments are shown schematically in Fig. 1. The jet flame burner consists of a circular well-contoured nozzle of 5mm in diameter, from which high purity methane emerges. The nozzle wall is contoured with fifth order polynomial profiles, and the area contraction ratio is 400. The nozzle exit shows a top-hat velocity profile, and the turbulence intensity at the centerline is about 0.5%. The whole jet flame system is placed inside an anechoic room in which a low-power, low-noise fan expelled exhaust. A typical case, based upon past experience [7], with an exit velocity of 11 m/s is chosen for the present study. Acoustic excitation is used to perturb the flow and to control the lifted flame stabilization. A pair of loud speakers with a flat response up to 30kHz is used for excitation. The resulting acoustic waveform intensity and the uniformity at the nozzle exit are carefully examined by a probe microphone (B&K 4182). Throughout the experiments, the speaker output waveform is properly maintained at 105 db. The spectral characteristics of the flow, in terms of the fundamental frequency and its sub-harmonics and harmonics, are measured by using the hotwire anemometer and the spectral response of the flame base to the flow and to the excitation is measured by an ionization probe. The fundamental frequency is 1200Hz and is

used for excitation. In order to resolve the stabilization behavior in a cycle of the lifted flame under acoustic excitation, an external triggering unit is designed to trigger the measurement instruments at a prescribed phase using the excitation sine wave from the function generator as the reference.

For the UV Raman system, the KrF excimer laser tuned to 248.56 nm, Stokes Raman signals from the sample volume are collected and focused by a Cassegrain optics (magnification ratio 2.34) through a 10 mm thick butyl acetate liquid filter. Two spectrometers, a 0.275m, f/3.8 spectrometer (SpectraPro-275) and a 0.5m, f/4 spectrometer (SPEX-500M) equipped with intensified CCD cameras (Princeton Instruments, 576 x 384 array) are used for monitoring the Stokes Raman and fluorescence signals. The spectral coverage of the 0.275 m spectrometer is 36.3 nm, which is sufficient to measure all the major species of Raman signals in methane flames. The 0.5 m spectrometer with 13.8nm spectral coverage is used to accurately resolve the CO<sub>2</sub>, O<sub>2</sub>, CO, and N<sub>2</sub>. In the current line Raman system, the camera image of the laser line, 3.31 mm in length which is determined by the effective width of the CCD chip (7.8 mm) and the magnification of the collection optics, is divided into eight segments in postprocessing, each with a spatial resolution of 0.41 mm.

## Result and Discussion

Figure 2 shows the general stability behavior of the current methane jet diffusion flame in terms of liftoff height and flame length as the exit velocity is increased. In the figure, the originally attached flame lifts off roughly at a velocity of 32m/s, the liftoff velocity, and blows out at about 70m/s, the blowout velocity. The lifted flame will remain if one reduces the exit velocity until about 11m/s, called the reattachment velocity, then the flame becomes reattached. With these three characteristic velocities, the stability behavior of the flame can be divided into three characteristic regions: the attachment, the hysteresis and the liftoff regions. It has been shown [2, 7] that acoustic excitation at the fundamental frequency of the jet flow will effectively organize the upstream fuel jet flow of the lifted flame in the hysteresis region into continuous periodic vortices. The periodic vortices due to the acoustic excitation and the dynamic movement of flame base can be monitored individually by microphone and ion probe. The data grabbed by A/D converter from microphone and ion probe are process using FFT (Fast Fourier Transform) method and shown in Fig. 3. The spectrum shows that the spectral response of the flame base follows closely to the spectral behavior of the upstream flow.

Constant-contour plots of mixture fraction, based on Bilger's definition [8], and OH mole fraction calculated from phase-averaged Raman data are depicted in Fig. 4 for regions near the flame base for the four characteristic phase angles. The visible flame base images of different phases can be captured by a triggered CCD (Charge Couple Device) with a 1/10000sec shutter and then digitalized by the frame grabber. The phase-averaged mean flame-base location and its standard deviation are analyzed using image processing from 100 images of each phase. The visible mean liftoff height of the flame varies with the phase angle of the excitation sine wave, and is compared with the mean liftoff height defined by OH concentration in Fig. 5. The results from visible flame images are consistent with OH concentration measured by Raman. The discrepancy at 270 degree may be due to error of low radiation of methane flame and uncertainty of Raman measurement. The result of flame base propagation and recession in a cycle is similar to that found by Lin et al [2] and Chao and Jeng [7] using the ionization probe. The results of Fig. 3 and Fig. 5 also imply good flame response to excitation under current excitation conditions.

The constant contour plots of H<sub>2</sub>O and OH mass fractions are shown for the two typical phase angles, 0 and 180 degrees, in Fig. 6. Significant amount, much higher than the mole fraction in ambient air, of H<sub>2</sub>O is found upstream of the flame base for both phase angles. The upstream H<sub>2</sub>O mole fraction for the 0 degree case is higher than that for the 180 degree case. Similar to that described in the large scale mixing model by Broadwell et al. [3] that combustion products brought to the edge of the flame are reentrained to mix with fresh reactant by large scale structures. The different H<sub>2</sub>O mole fractions found in different phase angles can be related to the “brought to the edge” and “reentrained” processes of the hot products due to the vortex evolution in a cycle.

The mixture fraction profile from the line Raman data is further used to calculate the scalar dissipation rate, which is defined as  $2D(\partial f/\partial x_j)$ , where  $D$  is the binary diffusivity and  $f$  is the mixture fraction. Constant contours for OH mole fraction and scalar dissipation rate for four typical phase angles are shown in Fig. 7. As expected, when the flame propagates upstream at the phase angle of 180 degree, the scalar dissipation rate around the flame base is relatively low as compared with that of other phase angles. At 180 degree the flame base is seen to propagate in a low dissipation environment. Everest et al. [9] based on the simulation of Ashurst and Williams [10] experimentally mapped the mixture fraction fields of the upstream cold jet flow without reaction. Their results showed that extensive strain, indicated by large dissipation rate, in the downstream portion of the large-scale vortex engulfment is associated with the thinning of the flammable layer and probably leading to extinction; whereas compressive strain of low dissipation rate in the upstream portion of the vortex engulfment thickens the flammable layer and in favor of flame propagation. Apparently, the current flame Raman results in Figs. 4 and 7 can further substantiate their cold flow results. Referring back to Fig. 4, the flammable layer, indicated by the mixture fraction between 0.03223 and 0.08339, upstream of the flame base becomes thinner at 0 degree and much thicker at 180 degree. In the meanwhile, in Fig. 7, the scalar dissipation rate upstream of the flame base becomes larger at 0 degree and smaller at 180 degree. Nevertheless, the current scalar dissipation rate calculated from Raman data, typically about  $0.3 \text{ s}^{-1}$  at the flame base, is much smaller than the value reported by Everest et al. [9], as high as  $450 \text{ s}^{-1}$  instantaneous and  $6.8 \text{ s}^{-1}$  mean, and the estimated extinction value of  $7.8 \text{ s}^{-1}$  from the strain rate relation by Peters and Williams [12]. Therefore, a new model of the stabilization mechanism of a lifted flame is proposed and depicted schematically in Fig. 8 that in a fundamental excitation cycle, the evolution of the large scale vortex located immediately upstream of the lifted flame first induces extensive strain and large dissipation rate involving thinning of the flammable layer on the flame and the flame becomes weak with probable local extinction as the vortex rotates and moves downstream. Then on the other half of the cycle, the evolution of the vortex induces compressive strain with low dissipation rate and thick flammable layer facilitating flame propagation.

## Conclusion

Detailed phase-averaged line Raman and visualization measurements are performed to delineate the stabilization process of a lifted methane diffusion flame slightly tuned by acoustic excitation. Phase averaging using the excitation wave as the reference is employed to process the data. Good flame response to excitation is found under current excitation conditions. Similar to Tacke et al.'s finding[13], the flame base is found to locate in lean mixtures for all the phase angles. Combustion products are found upstream of the flame base.

This result supports Broadwell et al.'s large-scale reentrainment model. The current flame Raman results of mixture fraction and scalar dissipation rate can further substantiate Everest et al.'s cold flow results and Ashurst and Williams's simulation and extend to the flame stabilization behavior. A model for the stabilization process of a lifted flame in an oscillation cycle is proposed, that can be described by the evolution of the upstream large-scale vortex, the induced strain and dissipation rate on the flammable layer and the flame base.

## Reference

1. Vanquickenborne, L., and van Tigglen, A., *Combust. Flame* 10:59-69 (1966).
2. Lin, C.K., Jeng, M.S., and Chao, Y.C., *Exp. in Fluids* 14:353-365 (1993).
3. Broadwell, J.E.E., Dahm, W.J.A., and Mungal, M.G., *Twentieth Symposium (International) on Combustion*, The Combustion Institute, Pittsburgh, 1984, pp. 303-310.
4. Gollahalli, S.R., Savas, Ö., Huang, R.F., and Rodriguez Azara, J.L.R., *Twenty-First Symposium (International) on Combustion*, The Combustion Institute, Pittsburgh, 1986, pp. 1463-1469.
5. Pitts, W.M., *Twenty-Third Symposium (International) on Combustion*, The Combustion Institute, Pittsburgh, 1990, pp. 661-668.
6. Schefer, R.W., Namazian, M., and Kelly, J., *Combust. Flame* 99:75-86, (1994).
7. Chao, Y.C., and Jeng, M.S., *Twenty-Fourth Symposium (International) on Combustion*, The Combustion Institute, Pittsburgh, 1992, pp. 333-340.
8. Bilger, R.W., *Twenty-Second Symposium (International) on Combustion*, The Combustion Institute, Pittsburgh, 1988, pp. 475-482.
9. Everest, D.A., Feikema, D.A., and Driscoll, *Twenty-Sixth Symposium (International) on Combustion*, The Combustion Institute, Pittsburgh, 1996, pp. 129-136.
10. Everest, D.A., Feikema, D.A., and Driscoll, *Twenty-Sixth Symposium (International) on Combustion*, The Combustion Institute, Pittsburgh, 1996, pp. 129-136.
11. Ashurst, W.T., and Williams, F.A., *Twenty-Sixth Symposium (International) on Combustion*, The Combustion Institute, Pittsburgh, 1990, pp. 543-550.
12. Peters, N., and Williams, F.A., *AIAA J.* 21: 423-429, (1983).
13. Tacke, M.M., Geyer, D., Hassel, E.P., and Janicka, J., *Twenty-Seventh Symposium (International) on Combustion*, The Combustion Institute, Pittsburgh, 1998, pp. 1157-1165.

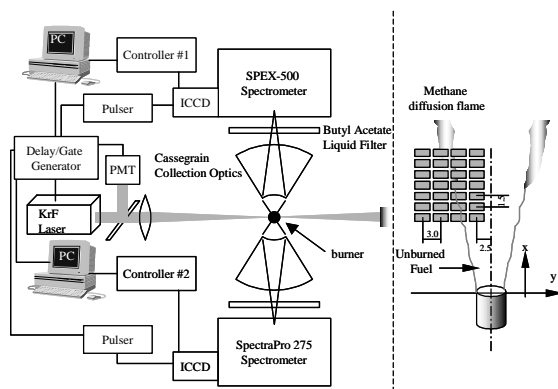


Fig 1. Schematic of the experimental setup, and Raman systems, and the measurement locations for the line Raman segments.

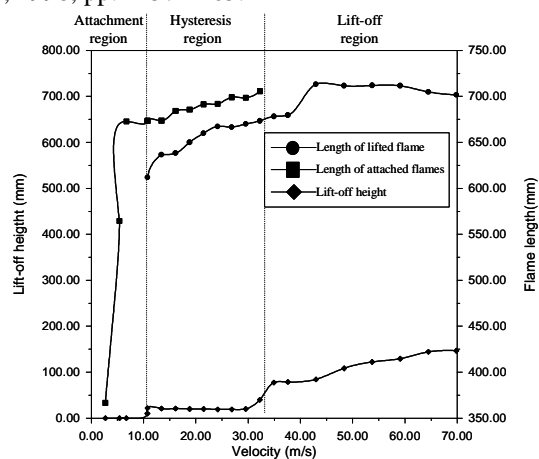


Fig 2. The flame length and liftoff height as a function of exit velocity for the methane jet diffusion flame in the attachment, hysteresis, and lift-off regions

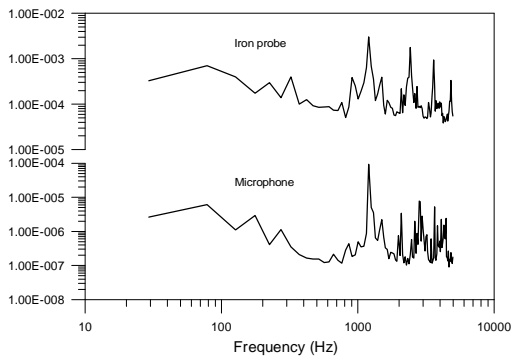


Fig 3. The frequency spectrum of flame base periodic propagation and acoustic excitation

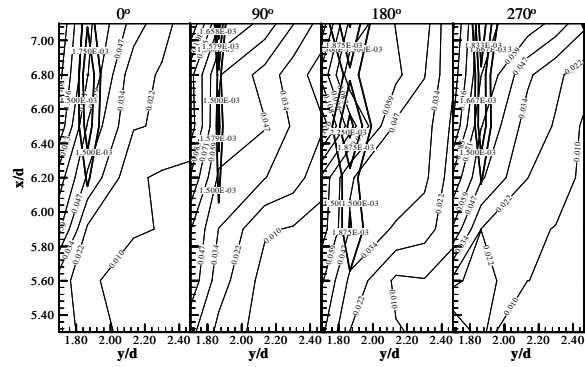


Fig 4. Constant contour plot of OH mole fraction and mixture fraction. Bold line: OH mole fraction; thin line: mixture fraction.

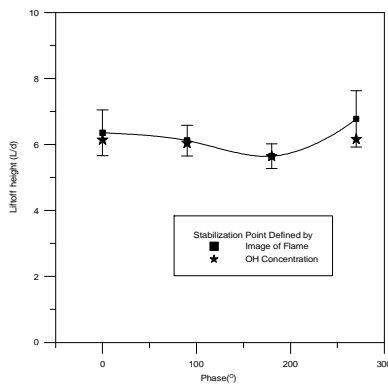


Fig 5. Phase averaged mean lift off height of the visible flame and flame base defined by OH concentration varies with the phase angle of sine wave acoustic

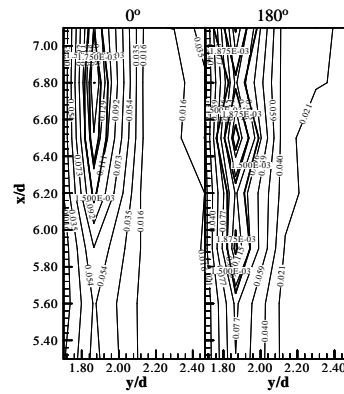


Fig 6. Constant contour plot of OH mole fraction and H<sub>2</sub>O mole fraction for the phase angle at 0 degree and 180 degree; bold line: OH mole fraction; thin line: H<sub>2</sub>O mole fraction.

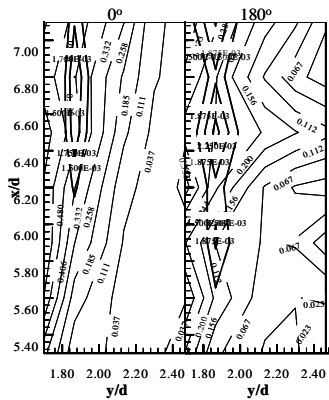


Fig 7. Constant contour plot of OH mole fraction and scalar dissipation rate for two phase angles; bold line: OH mole fraction; thin line: dissipation rate.

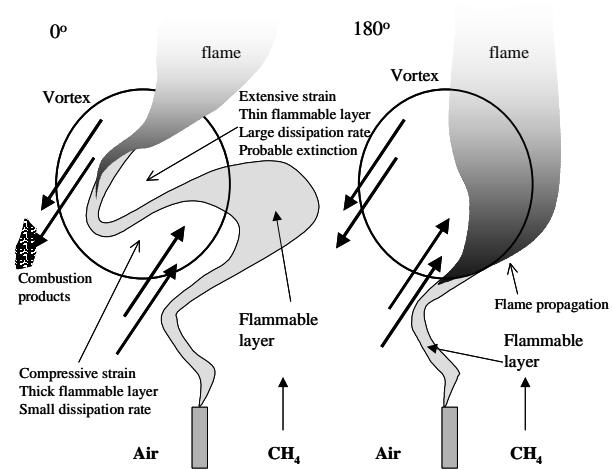


Fig 8. Schematic showing the flame behavior in the stabilization process of the lifted diffusion flame.